Topological grounds for challenging behavior of the heavy-fermion metal $\beta - YbAlB_4$ under the application of magnetic field and pressure

V. R. Shaginyan,[1,2,*] A. Z. Msezane,[2] K. G. Popov,[3,4] J. W. Clark,[5,6] V. A. Khodel,[7,5] and M. V. Zverev[7,8]

[1]*Petersburg Nuclear Physics Institute, NRC Kurchatov Institute, Gatchina, 188300, Russia*
[2]*Clark Atlanta University, Atlanta, GA 30314, USA*
[3]*Komi Science Center, Ural Division, RAS, Syktyvkar, 167982, Russia*
[4]*Department of Physics, St.Petersburg State University, Russia*
[5]*McDonnell Center for the Space Sciences & Department of Physics, Washington University, St. Louis, MO 63130, USA*
[6]*Centro de Ciências Matemáticas, Universidade de Madeira, 9000-390 Funchal, Madeira, Portugal*
[7]*NRC Kurchatov Institute, Moscow, 123182, Russia*
[8]*Moscow Institute of Physics and Technology, Dolgoprudny, Moscow District 141700, Russia*

We analyze the thermodynamic properties of $\beta - YbAlB_4$, explain their scaling behavior, the NFL behavior and its frailness with respect to the application of magnetic field B, and demonstrate a good elucidation of experimental facts within the framework of the fermion condensation theory. Then, we explain the ability of the thermodynamic properties and the anomalous temperature T dependence of the electrical resistivity $\rho \propto T^{3/2}$ to cope with the application of pressure P. To illuminate the observed behavior, we construct the schematic $T - B$ and $T - P$ phase diagrams.

PACS numbers: 71.27.+a, 71.10.Hf, 72.15.Eb

Recently, the striking measurements under the application of both magnetic field B and hydrostatic pressure P on the heavy-fermion (HF) metal $\beta - YbAlB_4$ have been performed and theoretically analyzed, see e.g.[1–11] The measurements of the magnetization $M(B)$ at different temperatures T show that the magnetic susceptibility $\chi = M/B \propto T^{-1/2}$ demonstrates the non-Fermi liquid (NFL) behavior, and diverges at temperature $T \to 0$, implying that the quasi-particles effective mass M^* diverges as $M* \propto B^{-1/2} \propto T^{-1/2}$ at the quantum critical point (QCP).[2] Such a quantum criticality is commonly attributed to the scattering of electrons off quantum critical fluctuations related to a magnetic instability. In a single crystal of $\beta - YbAlB_4$, QCP is well located away from a possible magnetic instability.[2] Furthermore, it is observed that QCP is robust against P, that is under the application of P the divergent T and B dependences of χ is conserved and accompanied by anomalous $T^{3/2}$ dependence of the electrical resistivity ρ.[6] In contrast, under the application of a tiny magnetic field B the divergences are suppressed, resulting in the Landau-Fermi liquid (LFL) behavior at low temperatures.[1,2] As a result, we have to deal with a challenging problem including on one hand an explanation of the fragile NFL behavior in magnetic fields, and on the other hand, the robustness of the NFL behavior against the application of pressure P in zero magnetic field.

In this communication we analyze the thermodynamic properties of $\beta - YbAlB_4$, explain their scaling behavior, the NFL behavior and its frailness with respect to the application of magnetic field $B||c$, and demonstrate a good elucidation of experimental facts within the framework of the fermion condensation (FC) theory. Then, we explain the ability of the thermodynamic properties and anomalous $T^{3/2}$ dependence of the electrical resistivity ρ to cope with the application of the pressure. To illuminate the observed behavior, we construct the schematic $T - B$ and $T - P$ phase diagrams.

We start with elucidation of the scaling behavior of the thermodynamic functions of HF compounds within the framework of HF homogeneous liquid.[12–14] The Landau functional $E(n)$ depends on the quasiparticle distribution function $n_\sigma(\mathbf{p})$, where $\mathbf{p}$ is the momentum. Near the fermion condensation quantum phase transition (FCQPT), the effective mass M^* is governed by the Landau equation[12,13,15]

$$\frac{1}{M^*(T,B)} = \frac{1}{M^*(T=0,B=0)} + \frac{1}{p_F^2}\sum_{\sigma_1}\int \frac{\mathbf{p}_F\mathbf{p_1}}{p_F} F_{\sigma,\sigma_1}(\mathbf{p_F},\mathbf{p}_1)\frac{\partial \delta n_{\sigma_1}(T,B,\mathbf{p}_1)}{\partial \mathbf{p}_1}\frac{d\mathbf{p_1}}{(2\pi)^3}, \quad (1)$$

Here we have rewritten the quasiparticle distribution function as $\delta n_\sigma(\mathbf{p}) \equiv n_\sigma(\mathbf{p},T,B) - n_\sigma(\mathbf{p},T=0,B=0)$. The sole role of the Landau interaction $F(\mathbf{p_1},\mathbf{p_2}) = \delta^2 E/\delta n(\mathbf{p_1})\delta n(\mathbf{p_2})$ is to bring the system to FCQPT point, where $M^* \to \infty$ at $T = 0$, and the Fermi surface alters its topology so that the effective mass acquires temperature and field dependences, while the proportionality of the specific heat C/T and the magnetic susceptibility χ to M^* holds: $C/T \sim \chi \sim M^*(T,B)$. Near FCQPT the effective mass $M^*(T=0,B=0) \to \infty$, and Eq. (1) becomes homogeneous with $M^*(T=0,B) \propto B^{-z}$ and $M^*(T,B=0) \propto T^{-z}$, with the exponent z depending on the analytical properties of F.[12–14,16] On the ordered side of FCQPT at $T = 0$, the single particle spectrum $\varepsilon(\mathbf{p})$ acquires a flat part at the Fermi surface p_F

$$\varepsilon(\mathbf{p}) = \mu \quad (2)$$

over the region $p_i < p_F < p_f$, with μ being the chemical potential. At FCQPT the flat part shrinks, so that

$p_i \to p_F \to p_f$, and $\varepsilon(\mathbf{p})$ possesses an inflection point at p_F. As a result, $\varepsilon(\mathbf{p} \simeq \mathbf{p_F}) - \mu \simeq (p - p_F)^3$. Another inflection point emerges in the case of non-analytical Landau interaction F:

$$\varepsilon - \mu \simeq -(p_F - p)^2, p < p_F;\ \varepsilon - \mu \simeq (p - p_F)^2, p > p_F. \quad (3)$$

Accordingly, at the inflection point (3) the effective mass diverges as $M^*(T \to 0) \propto T^{-1/2}$. These specific features of ε can be used to separate the solutions of Eq. (1), corresponding to specific experimental situation. Namely, the experiment on $\beta - YbAlB_4$ shows that near QCP at $B \simeq 0$, the magnetization $M(B) \propto B^{-1/2}$,[1–11] and such a behavior of the magnetization corresponds to the spectrum $\varepsilon(\mathbf{p})$ given by Eq. (3) with $(p_f - p_i)/p_F \ll 1$. At finite B and T near FCQPT, the solutions of Eq. (1), defining the T and B dependents of $M^*(T, B)$, can be well approximated by a simple universal interpolating function.[12–14] The interpolation occurs between the LFL ($M^* \propto a + bT^2$) and NFL ($M^* \propto T^{-1/2}$) regimes, separated by the crossover region at which M^* reaches its maximum value M^*_M at temperature T_M, and represents the universal scaling behavior of $M^*_N(T_N)$

$$M^*_N(T_N) = \frac{M^*(T,B)}{M^*_M} = \frac{1+c_2}{1+c_1}\frac{1+c_1T_N^2}{1+c_2T_N^{5/2}}, \quad (4)$$

where c_1 and c_2 are fitting parameters, and $T_N = T/T_M$ is the normalized temperature. Here,

$$M^*_M \propto B^{-1/2}, \quad (5)$$

while

$$T_M \propto B^{1/2} \text{ and } T_M \propto B. \quad (6)$$

It follows from Eqs. (4), (5) and (6) that the effective mass exhibits the universal scaling behavior

$$M^*(T,B) = c_3\frac{1}{\sqrt{B}}M^*_N(T/B), \quad (7)$$

with c_3 is a constant.[12–14] Below Eqs. (4), (5), (6), and (7) are used along with Eq. (1) to describe the experiment in $\beta - YbAlB_4$. We note, that the scaling behavior takes place at temperatures $T \lesssim T_f$, where T_f is the temperature at which the influence of QCP vanishes.[12,13]

Taking into account Eq. (7), we conclude the magnetization M exhibits the scaling behavior, for it is given by

$$M(T,B) = \int \chi(T,B_1)dB_1 \propto \int \frac{M^*_N(T/B_1)}{\sqrt{B_1}}dB_1. \quad (8)$$

We obtain that at $T < B$ the system demonstrates the LFL behavior, at which $M(B) \propto B^{-1/2}$. At $T > B$, the system enters NFL region and $M(T) \propto T^{-1/2}$. While $dM(T,B)/dT$ again exhibits the scaling behavior, with $dM(T,B)/dT \propto T$ at $T < B$, and $dM(T,B)/dT \propto T^{-3/2}$ at $T > B$. Our analytical calculations are in accordance with the experimental facts[2,4,5], and free from fitting parameters and empirical functions. To confirm our analysis of the scaling behavior, we display in Fig. 1 our calculations of the dimensionless normalized magnetization $(B^{1/2}dM(T,B)/dT)_N$ versus the dimensionless normalized $(T/B)_N$. The normalization is carried out by dividing $B^{1/2}dM(T,B)/dT$ and T/B by the maximum value of $(B^{1/2}dM(T,B)/dT)_M$ and by $(B/T)_M$ at which the maximum value takes place. It is seen that the calculated single scaling function of the ratio $(T/B)_N$ follows the data over four decades of the normalized $(B^{1/2}dM(T,B)/dT)_N$, while the ratio itself varies over five decades. It also follows from Eq. (8) that $(B^{1/2}dM(T,B)/dT)_N$ exhibits the scaling behavior as a function of $(B/T)_N$. Figure 2 reports the scaling behavior $(B^{1/2}dM(T,B)/dT)_N$ of the archetypical HF metal $YbRhSi_2$. The solid curve representing the theoretical calculations is adopted from that depicted in Fig. 1. Thus, we see that the scaling behavior of $\beta - YbAlB_4$, extracted from measurements[17,18] and shown in Fig. 1, is not unique, and demonstrates the same crossover under the application of magnetic field in the wide range of the applied pressure, shown in the legend.

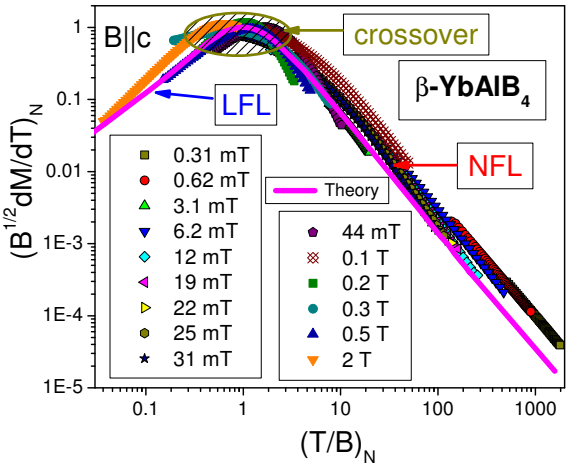

FIG. 1: (color online). The scaling behavior of the dimensionless normalized magnetization $(B^{1/2}dM(T,B)/dT)_N$ versus the dimensionless normalized $(T/B)_N$ at different magnetic fields B, shown in the legend. The data are extracted from measurements.[6] The LFL behavior, crossover and NFL as shown by the arrows. The theory is represented by the single scaling function.

Under the application of magnetic fields $B > B_{c2} \simeq 30$ mT and at sufficiently low temperatures, $\beta - YbAlB_4$ can be driven to the LFL state with its resistivity $\rho(T) = \rho_0 + AT^2$ with the coefficient A of the T^2 dependence. Measurements of the coefficient A produce information on its B-field dependence.[1] The $A(B)$ coefficient, being proportional to the quasiparticle–quasiparticle scattering cross-section, is found to be $A \propto (M^*(B))^2$.[19,20] This

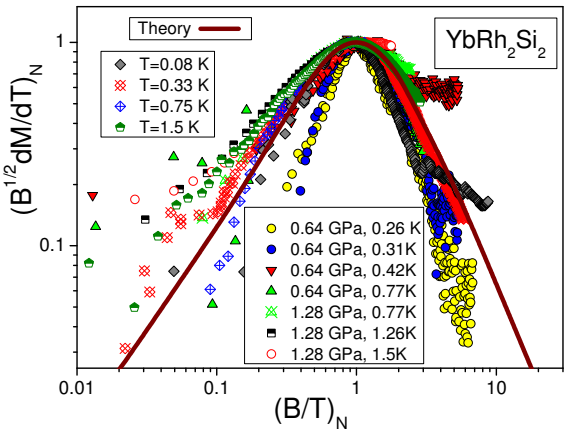

FIG. 2: (color online). The scaling behavior $(B^{1/2}dM(T,B)/dT)_N$ versus $(B/T)_N$ of the archetypical HF metal $YbRhSi_2$. The data are extracted from measurements of dM/dT versus B at fixed temperatures[17,18] The solid curve show the theoretical calculations, and is adopted from that depicted in Fig. 1. The applied pressures and temperatures are shown in the legends.

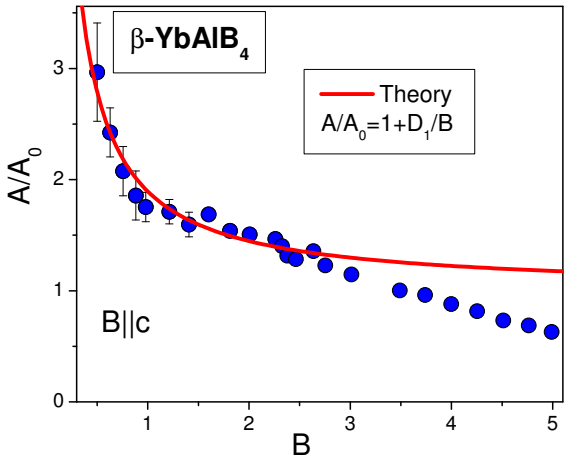

FIG. 3: (color online). Normalized coefficient $A(B)/A_0$ given by Eq. (10) as a function of magnetic field B shown by circles. D_N is the only fitting parameter. The experimental facts are extracted from measurements of $A(B)$.[1] Our calculations are shown by the solid curve.

implies in accordance with Eq. (5), that

$$A(B) \simeq A_0 + \frac{D}{B}, \tag{9}$$

where A_0 and D are fitting parameters.[12,13] We rewrite Eq. (9) in the reduced variable A/A_0

$$\frac{A(B)}{A_0} \simeq 1 + \frac{D_1}{B}, \tag{10}$$

where $D_1 = D/A_0$ is a constant. From Eq. (10) it is seen that $A(B)$ is reduced to a function depending on the single variable B. Figure 3 reports the fit of $A(B)$ to the experimental data[1], and displays good coincidence of the theoretical dependence (10) with the experimental facts. This means that the physics underlying the field-induced reentrance into the LFL behavior, is the same for classes of HF metals. We note, that deviations of the theoretical curve from the experimental points at $B > 2.5$ T are due to violation of the scaling at QCP.[5]

In Fig. 4, our calculations of $\chi(B) \propto M^*$ and $C/T = \gamma(B) \propto M^*$ are shown by the solid curve. Taking into account Eq. (5), that $A(B) \propto (M^*)^2$, and good description of χ and γ shown in Fig. 4, we verify Eq. (10), and conclude that the Kadowaki-Woods ratio $A/\gamma^2 \propto A/\chi^2 \simeq const$ is conserved in the case of $\beta - YbAlB_4$, being similar to that found in other heavy-fermion compounds.[1,3,12,21]

The above scaling properties permit to construct the schematic $T - B$ phase diagram of $\beta - YbAlB_4$, shown in Fig. 5, with the magnetic field B serving as control parameter. At $B = 0$, the system acquires the flat band,

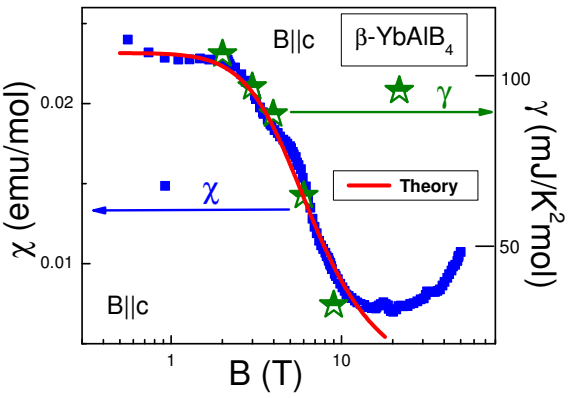

FIG. 4: (color online). The magnetic susceptibility $\chi = dM/dB = a_1 M_N^*$, the left axis, and the electronic specific heat coefficient $C/T = \gamma = a_2 M_N^*$, the right axis, versus magnetic field B.[5] Our calculations are depicted by the solid curve tracing the scaling behavior of M_N^* with a_1 and a_2 are fitting parameters.

given by Eq. (2) and corresponding to a strongly degenerate state, that is eliminated by the superconducting state.[12,22] The NFL regime reigns at elevated temperatures and fixed magnetic field. The magnetic-field-tuned QCP is indicated by the arrow and located at the origin of the phase diagram, since application of any magnetic field destroys the flat band and shifts the system into the LFL state, provided that the superconducting state were absent.[12,13,23] The hatched area denoting the crossover

that separates the NFL state from the LFL state, and contains the dashed line $T_M(B) \simeq B$, as it is shown in Fig. 1.

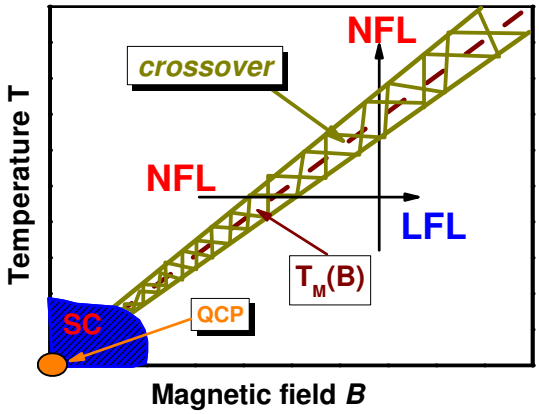

FIG. 5: Schematic $T-B$ phase diagram. The vertical and horizontal arrows show LFL-NFL and NFL-LFL transitions at fixed B and T, respectively. The hatched area separates the NFL phase and the weakly polarized LFL phase and represents the transition region. The dashed line in the hatched area represents the function $T_M \propto B$, see Eq. (6). The QCP located at the origin and indicated by the arrow denotes the quantum critical point at which the effective mass M^* diverges. QCP is covered by the superconducting phase labeled by SC.

The heavy-fermion metal $\beta-YbAlB_4$ is a superconductor on the ordered side of the corresponding phase transition. When analyzing the NFL behavior of $\rho(T)$ on the disordered side of this transition, one should have in mind that several bands simultaneously intersect the Fermi surface so that the HF band never covers the entire Fermi surface. Hence, it follows that quasiparticles that do not belong to the HF make the main contribution to the conductivity. Thus, the resistivity takes form $\rho(T) = M^*_{norm}\gamma(T)$, where M^*_{norm} is the averaged effective mass of normal quasiparticles and $\gamma(T)$ is their damping. The main contribution to $\gamma(T)$ can be estimated as $\gamma \propto T^2 M^*(M^*_{norm})^2$.[24–27] Taking into account Eqs. (3) and (6), we obtain $\rho(T) \propto T^{3/2}$.[27] On the other hand, one would expect that at $T \to 0$ the flat band (2) comes into play, making $\rho(T) \propto A_1 T$ whose magnitude A_1 is proportional to the flat band range $(p_f - p_i)/p_F \ll 1$. Such a behavior is not seen, for this aria is captured by the superconductivity, as it is seen from Fig. 5. The low-T resistivity $\rho(T, P = 0) \propto T^{3/2}$ found experimentally for the normal state of $\beta-YbAlB_4$ is consistent with this behavior.[6] When the pressure P is raised to a critical value P_c, it is found that around P_c the HF metal $\beta-YbAlB_4$ exhibits a crossover to Landau-like behavior $\rho(T) = \rho_0 + A_2 T^2$. Assuming that $P \propto x$, with x being the doping or the HF number density[28], we conclude that such behavior closely resembles the

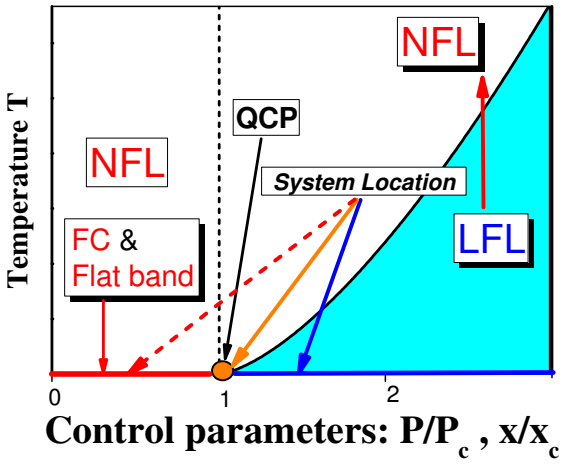

FIG. 6: Schematic $T-x$ phase diagram of system with FC. Pressure P/P_c and the number density x/x_c are taken as the control parameter. At $P/P_c < 1$ the system is shifted beyond QCP, and develops the flat band induced by FC. This location of the system is shown by the short dash arrow. At $P/P_c < 1$ and finite $T < T_f$ the system exhibits the NFL behavior. At $P/P_c > 1$ and sufficiently low temperatures, the system is in the LFL state as shown by the shadowed area. This location of the system is depicted by the arrows. The vertical arrow illustrates the system moving in the LFL-NFL direction along T at fixed control parameters.

NFL behavior $\rho(T) \propto T^{1.5\pm0.1}$ revealed in measurements of the resistivity in electron-doped high-T_c superconductors $La_{2-x}Ce_xCuO_4$.[29,30] In that case the effective mass $M^*(x)$ diverges when $x \to x_c$ or $P \to P_c$ [29,30]

$$(M^*(x))^2 \propto A \simeq \left(a_1 + \frac{a_2}{x/x_c - 1}\right)^2, \qquad (11)$$

where a_1 and a_2 are constants, and x_c is the critical doping at which the NFL behavior changes to LFL, for FC is decayed at x_c and the system transits to the disordered side of FCQPT.[12,13,27]

The schematic $T-x$ phase diagram of $\beta-YbAlB_4$, tuned by pressure P or by the number density x, is reported in Fig. 6. As seen from Fig. 6, at $P/P_c < 1$ (or $x/x_c < 1$) the system is located on the ordered side of topological phase transition, represented by FC-QPT, and demonstrates the NFL behavior at $T \lesssim T_f$. Thus, the NFL behavior, induced by FC that persists at $P < P_c$, is robust against application of pressure $P/P_c < 1$.[13,31] We note that such a behavior is observed in quasicrystals.[14,32] At low temperatures the FC state with flat band, shown by the arrow, is strongly degenerate. The degeneracy stimulates the emergence of different phase transitions, lifting it. The NFL state can be captured by different states such as superconducting (like that in $\beta-YbAlB_4$), or antiferromagnetic (like that in $YbRh_2Si_2$). At rising pressure, as it is shown

by the arrows, the system enters the region $P/P_c \geq 1$. At $P/P_c > 1$ the system is located before FCQPT, and demonstrates the LFL behavior at low temperatures. As a result, the system remains in the LFL region at sufficiently low temperatures, as it is shown by the shadowed area. The temperature range of this region shrinks as $P/P_c \to 1$, and M^* diverges as it follows from Eq. (11). These observations are in good agrement with experimental facts.[6]

In summary, we have analyzed the thermodynamic properties of $\beta - YbAlB_4$, and explained their scaling behavior. We have shown that NFL behavior is destroyed by the application of magnetic field. On the other hand, as we have explained, the thermodynamic properties and anomalous $T^{3/2}$ dependence of the electrical resistivity remain unchanged under the application of pressure $P < P_c$. We have also constructed the schematic $T - B$ and $T - P$ phase diagrams that are in good agreement with experimental facts.

VRS is supported by the Russian Science Foundation, Grant No. 14-22-00281. This work is partly supported by RFBR Grant No. 14-02-00044. AZM thanks the US DOE, Division of Chemical Sciences, Office of Energy Research, and ARO for research support. VAK and JWC acknowledge research support from the McDonnell Center for the Space Sciences, and JWC thanks the University of Madeira gracious hospitality during frequent visits.

* Electronic address: vrshag@thd.pnpi.spb.ru

[1] S. Nakatsuji, K. Kuga, Y. Machida, T. Tayama, T. Sakakibara, Y. Karaki, H. Ishimoto, S. Yonezawa, Y. Maeno, E. Pearson, G. G. Lonzarich, L. Balicas, H. Lee, and Z. Fisk, Nat. Phys. **4**, 603 (2008).
[2] Y. Matsumoto, S. Nakatsuji, K. Kuga, Y. Karaki, N. Horie, Y. Shimura, T. Sakakibara, A. H. Nevidomskyy, and P. Coleman, Science **331**, 316 (2011).
[3] Y. Matsumoto, K. Kuga, T. Tomita, Y. Karaki, and S. Nakatsuji, Phys. Rev. B **84**, 125126 (2011).
[4] Y. Matsumoto, S. Nakatsuji, K. Kuga, Y. Karaki, Y. Shimura, T. Sakakibara, A. H. Nevidomskyy, and P. Coleman, J. Phys.: Conf. Ser. **391**, 012041 (2012).
[5] Y. Matsumoto, K. Kuga, Y. Karaki, Y. Shimura, T. Sakakibara, M. Tokunaga, K. Kindo, and S. Nakatsuji, J. Phys. Soc. Jpn. **84**, 024710 (2015).
[6] T. Tomita, K. Kuga, Y. Uwatoko, P. Coleman, S. Nakatsuji, Science **349**, 506 (2015).
[7] A. H. Nevidomskyy and P. Coleman, Phys. Rev. Lett. **102**, 077202 (2009).
[8] A. Ramires, P. Coleman, A. H. Nevidomskyy, and A. M. Tsvelik, Phys. Rev. Lett. **109**, 176404 (2012).
[9] Y. Matsumoto, S. Nakatsuji, K. Kuga, Y. Karaki, Y. Shimura, T. Sakakibara, A. H. Nevidomskyy, and P. Coleman, J. Phys.: Conf. Ser. 391, 012041 (2012).
[10] S. Watanabe and K. Miyake, J. Phys. Soc. Jpn. **82**, 083704 (2013).
[11] S. Watanabe and K. Miyake, J. Phys. Soc. Jpn. **83**, 103708 (2014).
[12] V. R. Shaginyan, M. Ya. Amusia, A. Z. Msezane, and K. G. Popov, Phys. Rep. **492**, 31 (2010).
[13] M. Ya. Amusia, K. G. Popov, V. R. Shaginyan, V. A. Stephanovich, Theory of Heavy-Fermion Compounds, Springer Series in Solid-State Sciences **182**, (2014).
[14] V. R. Shaginyan, A. Z. Msezane, K. G. Popov, G. S. Japaridze, and V. A. Khodel, Phys. Rev. B **87**, 245122 (2013).
[15] L. D. Landau, Sov. Phys. JETP **3**, 920 (1956).
[16] V. A. Khodel, V. R. Shaginyan, and V. V. Khodel, Phys. Rep. **249**, 1 (1994).
[17] Y. Tokiwa, T. Radu, C. Geibel, F. Steglich, and P. Gegenwart, Phys. Rev. Lett. **102**, 066401 (2009).
[18] Y. Tokiwa, P. Gegenwart, C. Geibel, and F. Steglich, J. Phys. Soc. Jpn. bf 78, 123708 (2009).
[19] V.A. Khodel and P. Schuck, Z. Phys. B: Condens. Matter **104**, 505 (1997).
[20] P. Gegenwart, J. Custers, C. Geibel, K. Neumaier, K. T. T. Tayama, O. Trovarelli, and F. Steglich, Phys. Rev. Lett. **89**, 056402 (2002).
[21] K. Kadowaki and S. B. Woods, Solid State Commun. **58**, 507 (1986).
[22] V.A. Khodel, J.W. Clark, and M.V. Zverev, Phys. Rev. B **78**, 075120 (2008).
[23] V. R. Shaginyan, A. Z. Msezane, K. G. Popov, G. S. Japaridze, and V. A. Khodel, Europhys. Lett. **106**, 37001 (2014).
[24] V. A. Khodel and M. V. Zverev, JETP Lett. **85**, 404 (2007).
[25] V. R. Shaginyan, A. Z. Msezane, K. G. Popov, J. W. Clark, M. V. Zverev, and V. A. Khodel, Phys. Rev. B **86**, 085417 (2012).
[26] V. A. Khodel, V. R. Shaginyan, and P. Schuck, JETP Lett. **63**, 752 (1996).
[27] V. A. Khodel, J. W. Clark, K. G. Popov, and V. R. Shaginyan, JETP Lett. **101**, 413 (2015).
[28] Y. Tokiwa, P. Gegenwart, C. Geibel, and F. Steglich, J. Phys. Soc. Jpn. **78**, 123708 (2009).
[29] N. P. Armitage, P. Furnier, and R. L. Greene, Rev. Mod. Phys. **82**, 2421 (2010).
[30] K. Jin, N. P. Butch, K. Kirshenbaum, J. Paglione, and R. L. Greene, Nature, **476**, 73 (2011).
[31] V. R. Shaginyan, A. Z. Msezane, K. G. Popov, G. S. Japaridze, and V. A. Khodel, Europhys. Lett. **106**, 37001 (2014).
[32] K. Deguchi, S. Matsukawa, N. K. Sato, T. Hattori, K. Ishida, H. Takakura, and T. Ishimasa, Nature Materials **11**, 1013 (2012).